Experimental Investigation of a Variable Inertia Rotational Mechanism

Anika T. Sarkar[1], Carter A. Manson[1], and Nicholas E. Wierschem[1]

[1]Department of Civil and Environmental Engineering
Tickle College of Engineering

University of Tennessee, Knoxville, TN 37920

ABSTRACT
Recent advances in passive structural control systems have included devices that exploit nonlinear behavior. The explicit inclusion of nonlinearities allows these passive devices to be designed to have behavior and performance that varies with different load types and amplitudes. The variable inertial rotational mechanism (VIRM) is an example of a nonlinear passive control device and consists of a mechanism that converts linear motion into rotational motion and an attached flywheel that includes masses that can move radially inside the flywheel. The radial motion of the VIRM flywheel masses results in the flywheel moment of inertia continuously varying during the response of the device. Despite a potentially small physical mass, the VIRM can provide to a system large added mass effects that can vary greatly depending on the flywheel moment of inertia. The large and variable mass effects provided by the VIRM can significantly shift the natural frequency and reduce the response amplitude of an underlying structure. While the VIRM has been investigated numerically by a number of authors, the experimental study of these devices has been limited. Moreover, most of the studies have considered semi-active or active variable inertia flywheels. The investigation of passive VIRMs are rare. This study aims to address these gaps in knowledge and experimentally investigate the response modification and pseudo resonance frequency changes of an underlying structure produced by the VIRM considering different loading conditions. For this experimental investigation, a VIRM was designed and fabricated that utilizes a lead screw and a flywheel that contains masses connected to springs that can move radially in the flywheel. This VIRM was then attached to a single-degree-of-freedom structure and subjected to different excitation types using a shake table. With data from these experimental tests, the overall fundamental frequency and the response of the system was evaluated using the experimentally estimated system transfer functions. The results of this study shows that the inclusion of the VIRM reduces the response amplitude and significantly shifted the pseudo resonance frequency of the underlying structure and that these shifts in pseudo resonance frequency are highly dependent on the loading amplitude.

Keywords: Variable Inertia, Nonlinear, Shake Table Testing, Natural Frequency Shifts

INTRODUCTION

Inerters and inerter-based devices have been substantially studied during the last decade to overcome the limitations of conventional vibration mitigation strategies in civil engineering structures. The inerter is a linear two-terminal rotational inertial mechanism that generates a force proportional to the relative acceleration across its terminals. The inerter, like other rotational inertial mechanisms, converts translational motion into the rotational motion of a flywheel and, in the process of doing so, can create significant added mass effects.

Researchers have previously studied linear inerter-based devices that provide constant effective mass effects in structures. However, as the research advances, attention is paid to nonlinear rotational inertia mechanisms. The rotational inertia produced by these nonlinear devices can vary depending on the device's response. One example of a nonlinear device is the variable inertia rotational mechanism (VIRM), which has a moment of inertia that can change based on the rotational velocity of its flywheel.

In the VIRM, multiple symmetrically spaced masses are mounted inside the device’s flywheel using springs and guides, allowing radial mass movement within the guides. The vibration of the structure drives the ball-screw mechanism connecting the VIRM, which increases the absolute rotational velocity of the flywheel. When the flywheel rotational velocity decreases,

the masses move back toward their original position. Note that the flywheel rotational velocity is proportional to the relative velocity of the structure between the connection points of the VIRM.

Several researchers have recently investigated VIRMs to reduce the response amplitude of dynamic systems. In most studies, active and semi-active control mechanisms were used, and numerical simulations were primarily used for analysis [1]–[3]. The experimental investigation on passive VIRMs is also rare [4], [5]. Furthermore, limited research has been done to assess the effect of variable inertia on the natural frequency changes of the underlying structure.

This work experimentally explores the natural frequency changes of a base-excited single-degree-of-freedom structure (SDOF) with a VIRM. The SDOF structure is also tested, where the VIRM is replaced with a fixed inertia rotational mechanism (FIRM) and no flywheel to compare frequency changes and responses. Sine sweep excitations with various intensities are applied to it to understand the effect of the dynamically changing inertia of the VIRM on the structure's natural frequency change and response reduction.

This paper is structured as follows. The next section introduces the equations of motion (EOM) of the VIRM combined with a SDOF structure. The Experimental Setup section describes the designed test apparatus, instrumentation, and the loading considered. The Experimental Results section describes the test results, and the last section discusses the conclusions.

EOM OF VIRM ATTACHED TO A SDOF SYSTEM

In this study, a SDOF system attached to a VIRM is subjected to a ground motion $\left(\ddot{u}_g\right)$, as presented in

Figure 1. The VIRM is placed between the rigid mass (m_s) and the base and is parallel to the spring with stiffness (k_s) and a damper with viscous damping coefficient (c_s). The masses (m_{sd}) inside the flywheel are constrained such that they can move radially in the flywheel when the absolute rotational velocity $\left(\dot{\theta}\right)$ of the flywheel increases. The radial motion causes a restoring force (F_{bsd}) in the nonlinear springs, and the viscous dampers (c_{sd}) dissipate energy in the system. For the FIRM case, the masses are fixed at the initial position, x_0 in the flywheel frame and the nonlinear springs and the viscous dampers inside the flywheel are removed.

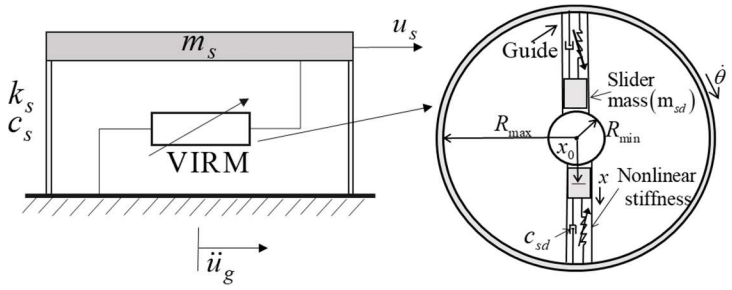

Figure 1. Schematic diagram of a SDOF primary system with VIRM (left), VIRM flywheel with two masses at their initial location (right)

The equations of motion of the VIRM combined system with primary system displacement relative to the ground, u_s, and slider radial displacement, x, and the primary system with the FIRM are expressed in Eq. (1) and (2), respectively,

$$\begin{aligned} &m_s\ddot{u}_s + J\alpha^2\left(\ddot{u}_s - \ddot{u}_g\right) + 2nm_{sd}x\dot{x}\alpha^2\dot{u}_s + nm_{sd}x^2\alpha^2\left(\ddot{u}_s - \ddot{u}_g\right) + c_s\dot{u}_s + k_s u_s = -m_s\ddot{u}_g \\ &m_{sd}\ddot{x} - m_{sd}x\alpha^2\dot{u}_s{}^2 + F_{bsd}\left(x\right) + c_{sd}\dot{x} = 0 \end{aligned} \tag{1}$$

$$m_s\ddot{u}_s + J\alpha^2\left(\ddot{u}_s - \ddot{u}_g\right) + nm_{sd}x_0{}^2\alpha^2\left(\ddot{u}_s - \ddot{u}_g\right) + c_s\dot{u} + k_s u = -m_s\ddot{u}_g \tag{2}$$

where J is the static rotational inertia and n is the number of slider masses in the VIRM/FIRM.

As seen from Eq. (2), the EOM of the system with a FIRM is linear; thus, the dynamic properties of this system should be constant. In contrast, Eq. (1) shows a nonlinear EOM for the system with a VIRM. The nonlinear components include a coefficient on an acceleration term that grows with increased slider radial position, as well as a complicated nonlinear term combining slider velocity, slider position, and primary system velocity. The nonlinear components of the VIRM EOM should result in dynamic properties that vary with the amplitude of the system response. Previous numerical studies have shown this system capable of apparent softening behavior [6]. The next sections of this work will experimentally investigate potential softening and vibration mitigation that results from the VIRM.

EXPERIMENTAL SETUP

A modified die set test apparatus with four springs is used to create a simplified SDOF environment. The reason behind using the die set is that die sets are precisely aligned and designed to primarily move along one axis, which helps to avoid any alignment issues arising from the oscillating system. The schematic configuration of the experimental setup is presented in Figure 2. This figure shows that springs connect the top and bottom mass plates. To align the two mass plates precisely, guide pins with guide bushings are used. Moreover, two adapter plates connect the VIRM flywheel to the primary structure with a lead-screw mechanism. Although the motion of the die set is configured to be limited to the vertical direction, some horizontal and torsional movement can be present in the structure.

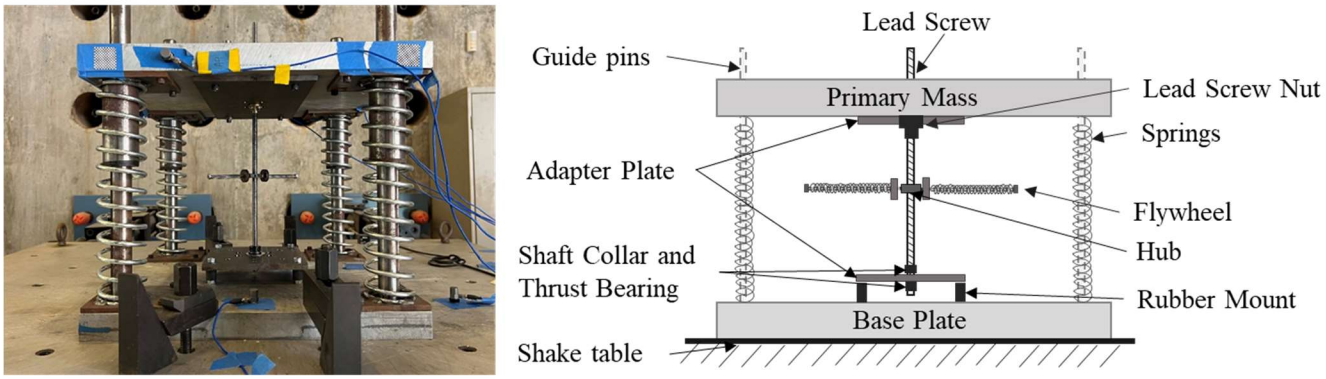

Figure 2. Experimental test setup (left), Schematic configuration of the structure with the VIRM (right)

The primary mass, m_s=17.92 kg, is an aluminum plate with dimensions of 18"x18"x1.25". The spring stiffness was selected such that the natural frequency of the structure without any rotational inertial components (lead screw or flywheel) is 5.3 Hz.

The modified die set was attached to the shake table, and eight PCB piezoelectric accelerometers were secured to both the die set and the shake table and were used to collect data with a sampling rate of 10240 Hz. One accelerometer was placed on the shake table measuring the input ground acceleration, and one was on the base plate of the structure measuring the transferred excitation. The rest of the accelerometers were placed on the top mass plate to ensure measurements in the x, y, and z directions. The die set was vertically excited by the shake table using forward sine-sweep signals in acceleration control along a frequency range of 1 Hz to 8 Hz for 90 seconds. Various percentages (10%, 20%, 30%, 40%, and 50%) of a baseline 0.1g acceleration amplitude sweep were applied to evaluate potential nonlinear structural behavior at different levels of excitation.

These tests were repeated with the VIRM replaced with a FIRM and with the experimental setup where the flywheel was removed and the lead screw remains connected to the die set, referred to as the no flywheel case. The decision to include the lead screw in the no flywheel case was made considering that much of the intrinsic damping in the setup comes from the passage of the lead screw through the lead screw nut. Thus, with the lead screw present in all cases, the differences resulting from each of the cases considered should primarily be due to the different mass effects provided by the devices. Note that in the no flywheel case, there will still be some added mass effects due to the rotational inertia of the lead screw, bearing, and shaft collars. Also, note that tests with the no flywheel case were not performed past 30% scaling of the loading due to the resulting large response amplitude in this case.

When the slider masses in the VIRM do not move in the flywheel, the rotational inertia provided by the VIRM is the same as the static rotational inertia of the FIRM. However, when the masses move inside the guide, the total flywheel moment of inertia consists of this static rotational inertia and a contribution from the changing radial position of the slider masses. Note that, the slider masses do not move beyond half the radius distance of the flywheel for the loads considered. In this study, inertance of the FIRM at initial position is 23 kg and the inertance of the VIRM when the masses are at the halfway position along the radius of the flywheel is 40 kg.

In this study, one accelerometer measuring in the vertical direction is focused on in the analysis to present the influence of different excitation amplitudes on the overall natural frequency change and the structure's response. To investigate the response in the frequency domain, this accelerometer reading and the measured ground acceleration are utilized to produce estimated frequency response functions (FRFs). The estimated FRFs are produced using Welch's average periodogram method which depends on factors such as, signal duration, window, number of points [7]. Each test was done five times to allow for averaging, a Hanning window was applied to each test data set to reduce spectral leakage, 0% overlap ratio was used, and the same number of points as one test is utilized in this estimation.

EXPERIMENTAL RESULTS

This section presents the experimental results for different amplitude swept sine loadings applied to the experimental setup described in the previous section. As discussed above, the results presented primarily consist of time histories of the vertical primary mass acceleration and FRFs showing the relationship between the applied vertical table acceleration and the vertical primary mass acceleration.

Figure 3 shows the vertical acceleration time history response of the primary structure for three different ground acceleration amplitudes. It can be observed that the acceleration response increases for higher excitation levels, and the peak response of the structure with no flywheel rises most rapidly as the excitation amplitude increases. The structure with no flywheel has the highest acceleration response for all excitation amplitudes compared to the structures with flywheels. The figure also shows that the structure with the FIRM has a lower response than the structure with no flywheel, but that the VIRM structure has the lowest acceleration response for all the excitation amplitudes considered.

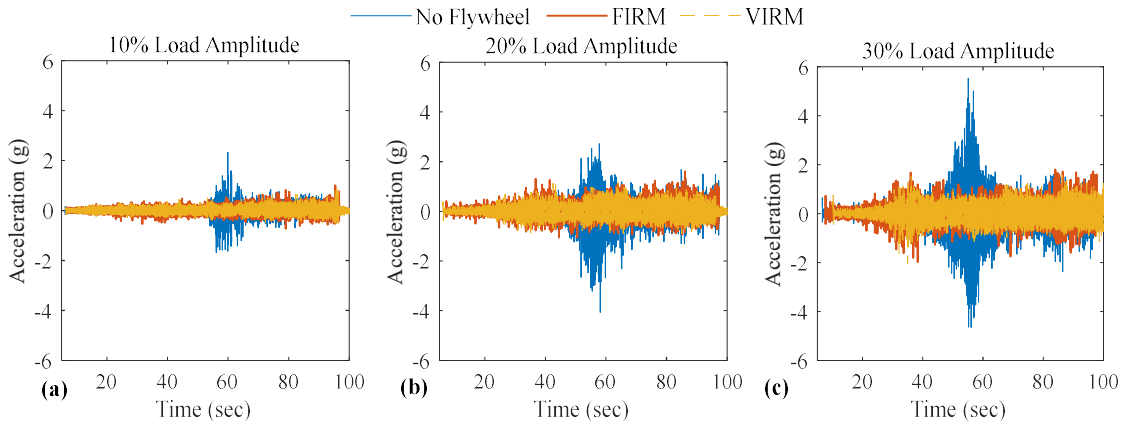

Figure 3. Acceleration time history of the primary structure for sine-sweep excitations with 3 different amplitudes: (a) 10% (b) 20% (c) 30%

The average root mean square (RMS) acceleration responses for the primary structure with no flywheel, FIRM and VIRM are presented in Table 1. These average RMS values were computed by averaging the resulting RMS values of the absolute acceleration from all of the individual tests with the same device and loading properties. The RMS value is significant as it provides a measure corresponding to the overall amplitude of the acceleration responses. Table 1 shows that the average RMS acceleration for all the structural configurations increase as higher scaling of load is applied to it. As no tests were done above 30% scaling of the baseline loading for the no flywheel case, there are no numerical values reported for those cases. The primary structure with no flywheel has the highest average RMS acceleration response compared to the FIRM and VIRM cases for all the loading amplitudes considered. It is observed that at low load amplitude, the average RMS of the FIRM and VIRM are the

same. For instance, at 10% and 20% load amplitude, the structure has the same average RMS acceleration of 0.08 g and 0.13 g with the FIRM and the VIRM, respectively. The similar response behavior of the FIRM and VIRM could be because at low load amplitudes, the masses in the VIRM stay close to the initial position. Hence, the VIRM behaves very similarly to the FIRM. As higher load amplitudes are applied to the structure, the average RMS acceleration is lower for the VIRM cases compared to the FIRM cases.

Table 1. Average RMS acceleration of the primary structure with no flywheel, VIRM and FIRM configurations at different loading amplitudes

		Average RMS acceleration (g)				
Load Amplitude		10%	20%	30%	40%	50%
Primary Structure Configurations	No Flywheel	0.11	0.27	0.39	-	-
	FIRM	0.08	0.13	0.18	0.21	0.24
	VIRM	0.08	0.13	0.17	0.19	0.23

FRFs relating the absolute acceleration response and ground acceleration input corresponding to the structure with no flywheel and the structure with the VIRM and the FIRM are shown in Figure 4. Although the tests were done for a sine sweep with frequency range between 1 Hz and 8 Hz, it can be observed in this figure that there is noise at low and high frequencies for all the load amplitudes, likely resulting from the windowing used, which impacts results at the beginning and end of the sweep more significantly. The pseudo resonance frequencies can be identified from this figure as the frequencies the peak values occur at, ignoring noise. This figure shows that the pseudo resonance frequency of the structure with no flywheel reduces when it is connected to a FIRM or VIRM flywheel and is the lowest when it is attached to the VIRM flywheel. For instance, at a 20% excitation amplitude, the pseudo resonance frequency of the structure with no flywheel, FIRM, or VIRM are 4.78 Hz, 2.81 Hz, and 2.69 Hz, respectively. Figure 4 also shows the frequency response behavior of the primary structure for different loading amplitudes. At 10% load amplitude, the structure with the VIRM or the FIRM has a very similar and low response amplitude across the frequency ranges. It is observed that the pseudo resonance frequency of the structure with no flywheel reduces with increasing excitation amplitude. The pseudo resonance frequency of the structure with no flywheel changes from 4.86 Hz to 4.75 Hz given an increase in load scaling from 10% to 30%. This behavior is not anticipated for the structure with no flywheel but it could be because at high levels of loading, the lead screw connection in the flywheel can provide some nonlinearities to the structure. It is also observed that the pseudo resonance frequency of the VIRM structure reduces at higher levels of loading. For example, when the excitation amplitude increases from 20% to 30%, the pseudo resonance frequency with the VIRM reduces from 2.69 Hz to 2.56 Hz.

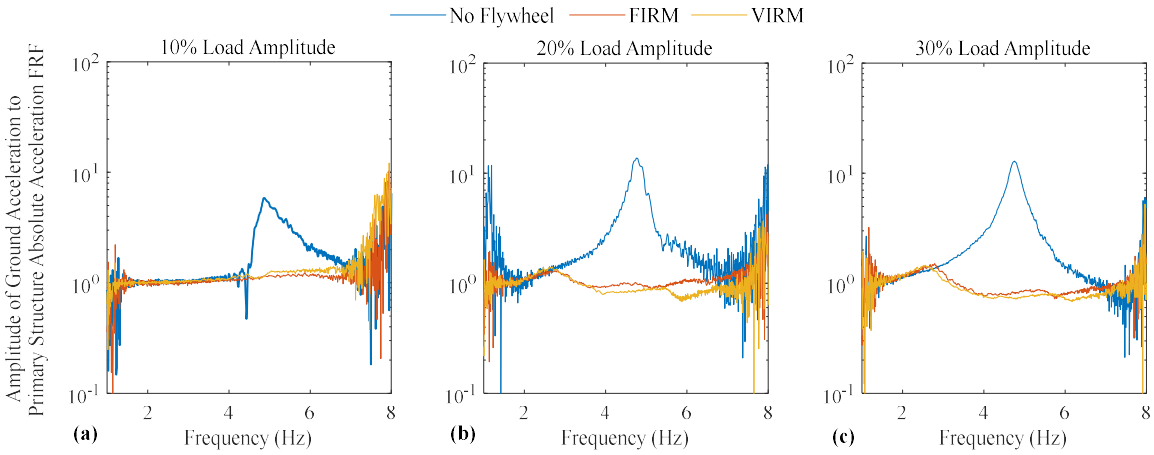

Figure 4. FRFs of the primary structure at different ground acceleration amplitudes: (a) 10% (b) 20% (c) 30%

The influence of the loading amplitude on the response modification and pseudo resonance frequency shifts is investigated with Figure 5 and Table 2. Table 2 lists the peak FRF values at the pseudo resonance frequencies. This table shows that these

peak values increase as higher load amplitude is applied for all the structure configurations. It also shows that the structure with no flywheel has the highest peak amplitude, as seen in Figure 4. Moreover, there is no beneficial reduction in the peak structure response amplitude when the FIRM is replaced with a VIRM at low load amplitudes, but there are some benefits at higher load amplitudes.

Table 2. Peak FRF (ground acceleration to absolute acceleration) value at pseudo resonance frequency for primary structure with no flywheel, VIRM, and FIRM configurations at different loading amplitudes

		Peak FRF value at Pseudo Resonance Frequency				
Load Amplitude		10%	20%	30%	40%	50%
Primary Structure Configurations	No Flywheel	5.81	13.77	12.87	-	-
	FIRM	1.15	1.33	1.50	1.52	1.60
	VIRM	1.23	1.37	1.44	1.47	1.56

Figure 5 shows FRFs relating the absolute acceleration response and ground acceleration input over a wider range of input amplitudes, 20% to 50%, and for the VIRM and FIRM only. Figure 5a shows that the FIRM's pseudo resonance frequencies are very similar for all the load conditions; for example, 2.81 Hz at 20% load amplitude and 2.76 Hz at 50% load amplitude. The slight difference in frequencies could be because of noise in the FRF estimate. Figure 5b shows that the pseudo resonance frequency reduces when the FIRM flywheel is replaced with a VIRM flywheel for all the loading amplitudes. The shift in natural frequency is because the slider mass movement in the VIRM flywheel increases the added effective mass in the structure. Hence, the additional effective mass reduces the natural frequency of the structure. This figure also shows that the peak FRF values increases and pseudo resonance frequency decreases as higher ground excitation is provided and large response results. For instance, the peak FRF amplitude increases from 1.37 to 1.56 and the pseudo resonance frequency reduces from 2.68 Hz to 2.33 Hz for an increase in ground excitation amplitude from 20% to 50% in the structure with the VIRM. Note that this shift in pseudo resonance frequency with increased amplitude is much larger than seen for either the no flywheel or FIRM cases.

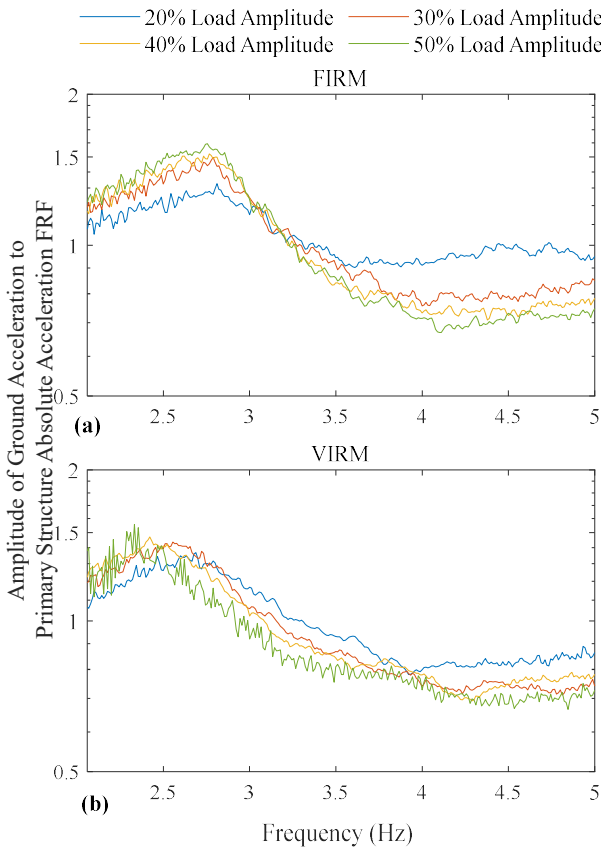

Figure 5. FRFs of the primary structure with the VIRM and the FIRM for 20%, 30%, 40% and 50% excitation amplitude

CONCLUSION

This paper experimentally investigates the dynamic behavior of a VIRM in a SDOF structure. In this paper, the structure is excited with a sine sweep ground motion. The results of this study show that the VIRM can notably reduce the pseudo-resonance frequency and response amplitude of the structure. The study also reveals that the variable rotational inertia can shift the pseudo resonance frequency with excitation amplitude. Overall, the paper suggests that the VIRM can affect structure dynamics and response significantly, although further research regarding various excitations, such as seismic ground motion, is necessary.

ACKNOWLEDGEMENTS

The research is sponsored by the National Science Foundation under Grant No. 1944513. The findings, opinions, recommendations, and conclusions in this paper are those of the authors alone and do not necessarily reflect the views of others, including the sponsors.

REFERENCES

[1] A. C. Mahato, S. K. Ghoshal, and A. K. Samantaray, “Influence of variable inertia flywheel and soft switching on a power hydraulic system,” *SN Appl. Sci.*, vol. 1, no. 6, p. 605, Jun. 2019, doi: 10.1007/s42452-019-0623-0.

[2] X. Dong, J. Xi, P. Chen, and W. Li, “Magneto-rheological variable inertia flywheel,” *Smart Mater. Struct.*, vol. 27, no. 11, p. 115015, Nov. 2018, doi: 10.1088/1361-665X/aad42b.

[3] P. Kushwaha, S. K. Ghoshal, and K. Dasgupta, “Dynamic analysis of a hydraulic motor drive with variable inertia flywheel,” *Proceedings of the Institution of Mechanical Engineers, Part I: Journal of Systems and Control Engineering*, vol. 234, no. 6, pp. 734–747, Jul. 2020, doi: 10.1177/0959651819875914.

[4] T. Xu, M. Liang, C. Li, and S. Yang, “Design and analysis of a shock absorber with variable moment of inertia for passive vehicle suspensions,” *Journal of Sound and Vibration*, vol. 355, pp. 66–85, Oct. 2015, doi: 10.1016/j.jsv.2015.05.035.

[5] S. Yang, T. Xu, C. Li, M. Liang, and N. Baddour, “Design, Modeling and Testing of a Two-Terminal Mass Device With a Variable Inertia Flywheel,” *Journal of Mechanical Design*, vol. 138, no. 9, p. 095001, Sep. 2016, doi: 10.1115/1.4034174.

[6] N. E. Wierschem, “Shift in Natural Frequencies of Structures with a Variable Inertia Rotational Mechanism,” presented at the Engineering Mechanics Institute Conference 2022, Baltimore, MD, USA, May 02, 2022.

[7] MathWorks, “Signal Processing Toolbox: User’s Guide (R2022a),” 2022. https://www.mathworks.com/help/pdf_doc/signal/signal.pdf (accessed Aug. 15, 2022).